



## ORIGINAL ARTICLE

# Analyzing the expressions for nanostructures via topological indices



Ying Wang<sup>a,b</sup>, Shamaila Yousaf<sup>c,d</sup>, Akhlaq Ahmad Bhatti<sup>c</sup>, Adnan Aslam<sup>e,\*</sup>

<sup>a</sup> Software Engineering Institute of Guangzhou, 510990 Guangzhou, China

<sup>b</sup> Institute of Computing Science and Technology, Guangzhou University, 510006 Guangzhou, China

<sup>c</sup> Department of Sciences and Humanities, National University of Computer and Emerging Sciences, Lahore Campus, B-Block, Faisal Town, Lahore, Pakistan

<sup>d</sup> Department of Mathematics, University of Gujrat, Hafiz Hayat Campus, Gujrat, Pakistan

<sup>e</sup> Department of Natural Sciences and Humanities, University of Engineering and Technology, Lahore (RCET), Pakistan

Received 23 August 2021; accepted 28 September 2021

Available online 8 October 2021

## KEYWORDS

Keywords;  
Chemical graph theory;  
Zigzag polyhex nanostructure;  
Topological indices

05C09;  
05C92

**Abstract** In molecular science, one of the key problem is to model a chemical compound and predict its chemical characteristic. Numerous hypothetical methods have been created by various analysts in this respect and one of them is concerned with the topological indices. A topological index is a numerical value attached with the structural graph of a molecule and is expected to predict certain chemical/physical properties of molecule [6]. Among the classes of topological indices, degree based topological indices play a vital role in chemical graph theory. In the current study, we compute the neighborhood second Zagreb index and the first extended first-order connectivity index of Planar zigzag nanotube  $PTUZC_6$ , polyhex zigzag nanotube  $H_2 = TUZC_6$ , polyhex zigzag nanotori  $TTUZC_6$ ,  $C_4C_8(S)[m, n]$  nanosheets,  $C_4C_8(S)[m, n]$  nanotubes,  $C_4C_8(S)[m, n]$  nanotori and arm-chair polyhex nanotubes  $TUAC_6[p, q]$ .

© 2021 The Author(s). Published by Elsevier B.V. on behalf of King Saud University. This is an open access article under the CC BY-NC-ND license (<http://creativecommons.org/licenses/by-nc-nd/4.0/>).

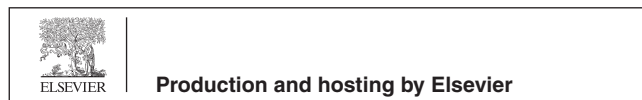
## 1. Introduction

Graph theory has played a significant role in chemistry in the last decades. Topological indices are essential in identifying the structures of chemical compounds. It is primarily a number associated with a chemical compound that has excellent features in chemistry. In quantitative structure–property relationship (QSPR) and quantitative structure–activity relationship (QSAR) studies, topological indices plays an important role. The QSAR and QSPR studies are undoubtedly of major importance in material sciences. Topological indices provide an overview of structural features of molecular graphs and reflects the physico-chemical properties of the activity/prop-

\* Corresponding author.

E-mail addresses: [wyang@mail.seig.edu.cn](mailto:wyang@mail.seig.edu.cn) (W. Yang), [shumaila.yousaf@uog.edu.pk](mailto:shumaila.yousaf@uog.edu.pk) (S. Yousaf), [akhlaq.ahmad@nu.edu.pk](mailto:akhlaq.ahmad@nu.edu.pk) (A.A. Bhatti), [adnanaslam15@yahoo.com](mailto:adnanaslam15@yahoo.com) (A. Aslam).

Peer review under responsibility of King Saud University.



erty under investigation (Randić, 1991; Tavakoli et al., 2013). To overview the structure–activity relationship, topological indices are required to effectively characterize structural features and bioactivity of chemical compounds (Balaban, 1979; Balaban et al., 1983; Balaban, 1988).

Let  $G$  be a finite, simple connected graph. In chemical graph theory, a molecular structure is a simple graph (a graph portraying chemical compounds) in which vertices correspond to the atoms and the edges corresponds to the bonds between the atoms. A numerical quantity of a chemical structure (molecular graph) which remains invariant under graph isomorphism is recognized as graph invariant. Topological index is an example of graph invariant. The most significant and widely used topological indices are degree-based topological indices. They have a remarkable application in mathematical chemistry.

For a vertex  $w \in V(G)$ , we use the notation  $N(w)$  for the set containing the vertices adjacent to  $w$ . The degree of a vertex  $w$  is the cardinality of the set  $N(w)$  and is denoted by  $d_w$ . Let  $S(w)$  denote the sum of degrees of the vertices adjacent to  $w$ . In other words,  $S(w) = \sum_{uv \in E(G)} d_u$  and  $N(t) = \{v \in V(G) | tv \in E(G)\}$ . For undefined terminologies related to graph theory, the author can read the following books (Gross and Yellen, 2000; Trinajstić, 1992; Godsil and Royle, 2001; Harary, 1969).

Consider the following general graph invariant

$$I(G) = \sum_{vw \in E(G)} f(S(v), S(w)).$$

Some special cases of the above invariants  $I$  have already been appeared in mathematical chemistry. For example, if we take  $f(S(v), S(w)) = S(v)S(w)$  and  $\frac{1}{\sqrt{S(v)S(w)}}$  then  $I$  gives neighborhood second Zagreb index (Réti et al., 2019) and the first extended first-order connectivity index (Bonchev and Kier, 1992; Toropov et al., 1997; Wang and Zhou, 2014; Zhou and Trinajstić, 2009), respectively. These indices are defined as:

$${}^1\chi_1(G) = \sum_{vw \in E(G)} \frac{1}{\sqrt{S_v S_w}}. \quad (1)$$

$$NM_2(G) = \sum_{uv \in E(G)} S(u)S(v). \quad (2)$$

In this paper we compute the first extended first-order connectivity index of polyhex zigzag nanotube  $TUZC_6$ , 2D lattice of polyhex zigzag nanotube and polyhex zigzag nanotori  $TTUZC_6$ . The same topological invariants are also computed for carbon nanosheet  $C_4C_8(S)[m, n]$ , carbon nanotube  $C_4C_8(S)[m, n]$ , carbon nanotori  $C_4C_8(S)[m, n]$  and armchair polyhex nanotubes  $TUAC_6[p, q]$ . Detail about theoretical and computation aspects of some families of carbon nanotubes can be view in (Eliasi and Salehi, 2008; Eliasi and Taeri, 2008; Eliasi and Taeri, 2008; Kanabur, 2018; Diudea et al., 2004; Monajjemi et al., 2008; Xiao et al., 2010; Editorial, 2007; Wang et al., 2001; Stover and Normile, 1993; Chakrabarty et al., 2015; Zhang et al., 2014; Qiad et al., 2014; Mahmiani et al., 2012; Farahani, 2012; Zhang et al., 2019; Zhang et al., 2020; Shao et al., 2018; Liu, 2021).

## 2. Motivation

Topological indices are useful to predict certain physical and chemical properties of the underline molecule. To check the chemical applicability of  ${}^1\chi_1$  and  $NM_2$ , we find their correlation coefficient with different physical/chemical properties of octane isomers. The values of acentric factor and entropy obtained from experiments and the computed values of  ${}^1\chi_1$  and  $NM_2$  for octane isomers are depicted in Table 1. The correlation coefficients between the entropy, acentric factor and  ${}^1\chi_1, NM_2$  are presented in Table 2. Observe that both the topological indices  ${}^1\chi_1$  and  $NM_2$  shows a very good correlation with entropy and acentric factor of octane isomers and thus can be used to predict these properties.

**Table 1** Values of Acentric factor, Entropy,  $NM_2$  and  ${}^1\chi_1$  of octane isomers.

Molecule	Acentric Factor	Entropy	$NM_2$	${}^1\chi_1$
2,2,3,3-Tetramethyl-butane	0.255294	93.06	217	0.068
2,4-Dimethyl-hexane	0.344223	106.98	121	0.091
2-Methyl-heptane	0.377916	109.84	98	0.101
2-Methyl-3-ethyl-pentane	0.332433	106.06	137	0.085
3-Ethyl-hexane	0.362472	109.43	115	0.093
2,2-Dimethyl-hexane	0.339426	103.42	132	0.087
3-Methyl-heptane	0.371002	111.26	106	0.097
2,3-Dimethyl-hexane	0.348247	108.02	129	0.088
2,5-Dimethyl-hexane	0.35683	105.72	113	0.094
2,2,4-Trimethyl-pentane	0.30537	104.09	147	0.082
4-Methyl-heptane	0.371504	109.32	107	0.096
3,3-Dimethyl-hexane	0.322596	104.74	148	0.082
3-Methyl-3-ethyl-pentane	0.306899	101.48	163	0.078
2,2,3-Trimethyl-pentane	0.300816	101.31	171	0.076
3,4-Dimethyl-hexane	0.340345	106.59	136	0.086
2,3,3-Trimethyl-pentane	0.293177	102.06	179	0.074
Octane	0.397898	111.67	84	0.104
2,3,4-Trimethyl-pentane	0.317422	102.39	151	0.081

**Table 2** The square of correlation coefficient of  $NM_2, {}^1\chi_1$  with entropy and acentric factor.

	$NM_2$	${}^1\chi_1$
Accentric factor	0.9708	0.9667
Entropy	0.8989	0.8418

One of the important use of topological indices is their discrimination power against octane isomers. The ability of discrimination of an index has applications within the coding and computer processing of molecular structures (isomers). The graphs of 18 octane isomers are depicted in Fig. 1. Let  $G_{p,q}$  be the number of edges in a graph  $G$  having end vertices of degree  $p$  and  $q$  respectively. Two graphs  $H$  and  $K$  are said to be edge equivalent iff  $H_{p,q} = K_{p,q}$ . Observe that the graph  $O_3$  and  $O_4$  are edge equivalent having different values of  ${}^1\chi_1$  and  $NM_2$  ( ${}^1\chi_1(O_3) = 0.097, {}^1\chi_1(O_4) = 0.096, NM_2(O_3) = 106$  and  $NM_2(O_4) = 107$ ). Similarly  $O_{11}$  and  $O_{12}$  are edge equivalent with different values of  ${}^1\chi_1$  and  $NM_2$  ( ${}^1\chi_1(O_{11}) = 0.086, {}^1\chi_1(O_{12}) = 0.087, NM_2(O_{11}) = 136$  and  $NM_2(O_{12}) = 137$ ). By using the definition, one can check that all the octane isomers have different values of  ${}^1\chi_1$  index. The same holds for  $NM_2$  index. Hence the discriminatory power of these indices is much better than other bond incident degree indices.

### 3. Results and Discussion

The most valuable nanomaterials available to scientists to achieve various experimentation and control objectives are carbon nanotubes(CNT). CNTs are important object to study because of their growing application in different fields especially in medical sciences. They have excellent features which include outstanding penetration capacity on the cellular membrane, strong drug load and therapeutic discharge capabilities dependent on pH. This make them fit for cancer and brain medications. CNTs as a medicine could attain great effectiveness, improve specificity and reduce side effects. Some investigations makes CNTs center of attention to treat and diagnose

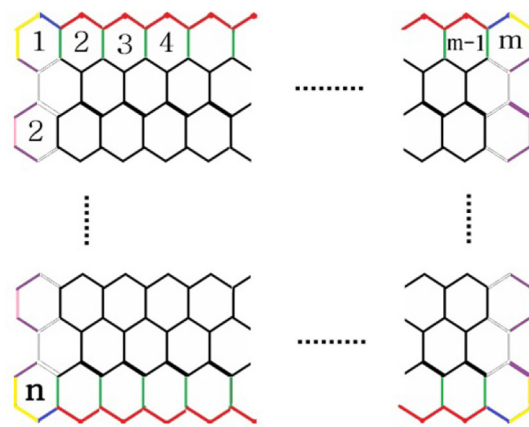


**Fig. 2** 2D structure of zigzag polyhex Lattice ( $PTUZC_6[m, n]$ ).

the central nervous system but the fundamental use of CNTs is in cancer treatment. (See Fig. 2).

#### 3.1. Results for Zigzag Polyhex Nanostructures

Graphene is a crystalline allotrope made from pure carbon atoms arranges in the form of two dimensional hexagonal lattice. It has unique properties containing best heat conductivity at room temperature and high optical transparency. zigzag polyhex lattice is a graphene lattice with  $m$  and  $n$  number of hexagons in each row and column respectively. We denote the graph of zigzag polyhex lattice by  $PTUZC_6$ . The graph

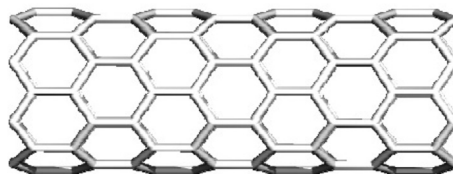


**Fig. 3** The 3D structure of polyhex zigzag nanotube ( $TUZC_6[m, n]$ ).

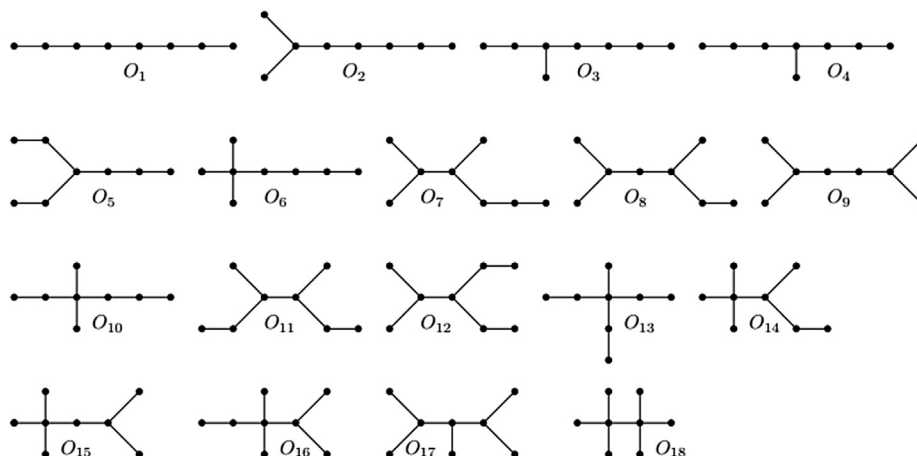


**Fig. 1** Graphs of Octane isomers.

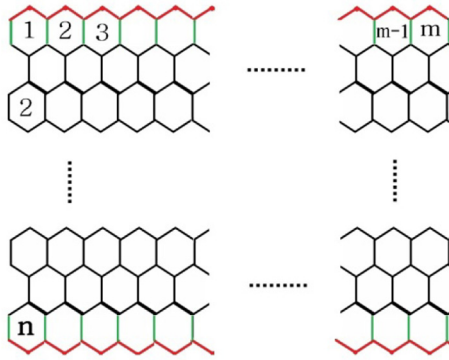


Fig. 4 2D structure of zigzag polyhex Lattice ( $PTUZC_6[m, n]$ ).



Fig. 5 The 3D structure of polyhex zigzag nanotori ( $TTUZC_6[m, n]$ ).

of  $PTUZC_6$  is depicted in Fig. 4. A zigzag polyhex nanotube denoted by  $TUZC_6[m, n]$  is obtained by rolling the graphene sheet into seamless tube such that vertical axis of the tube is parallel to the carbon-carbon bonds. We denote the Zigzag polyhex nanotorus by  $TTUZC_6[m, n]$  and is obtained by joining the two ends of zigzag polyhex nanotube. The graphs of  $TUZC_6[m, n]$  and  $TTUZC_6[m, n]$  are depicted in Fig. 3 and Fig. 5 respectively. The order and size of each of these nanostructures is shown Table 3.

In the next Theorems, we compute the two connectivity indices (neighborhood second Zagreb index and the first extended first-order connectivity index) for the famous nanostructure  $PTUZC_6[m, n]$ ,  $TUZC_6[m, n]$  and  $TTUZC_6[m, n]$ . For this we need to partition the edge set of each nanostructure depending on the sum of the degree of neighbors of the end vertices of each edge.

**Theorem 1.** Let  $G$  be the graph of zigzag polyhex lattice, then

$${}^1\chi_1(G) = \frac{7}{9}mn + (\frac{4}{\sqrt{42}} + \frac{2}{\sqrt{63}} - 1)m + (\frac{2}{\sqrt{10}} + \frac{2}{\sqrt{18}} - \frac{303}{180})n + \frac{4}{\sqrt{5}} + \frac{4}{\sqrt{35}} - \frac{2}{\sqrt{18}} - \frac{8}{\sqrt{42}} - \frac{4}{\sqrt{63}} - \frac{2}{\sqrt{10}} + \frac{39}{20}.$$

Table 3 Types of zigzag polyhex Nanostructures.

TypesofNanostructures	order	size
$PTUZC_6$	$2n(2m + 1)$	$6mn + n - m$
$TUZC_6$	$4mn$	$6mn - 4m$
$TTUZC_6$	$4mn$	$6mn$

Table 4 The edge partitions of  $PTUZC_6[m, n]$ .

$E_{p,q}$	Cardinality
$E_{4,5}$	8
$E_{5,5}$	$2n-4$
$E_{5,7}$	4
$E_{5,8}$	$4n-4$
$E_{6,7}$	$4m-8$
$E_{7,9}$	$2m-4$
$E_{8,8}$	$2n-2$
$E_{8,9}$	$4n-4$
$E_{9,9}$	$(m-3)(7n-9)$

$$NM_2(G) = 567mn - 1075n - 435m + 1223.$$

**Proof.** Let  $E_{p,q}(G)$  (or simply  $E_{p,q}$ ) denotes the set containing those edges  $e = uv$  of graph  $G$  such that  $S(u) = p$  and  $S(v) = q$ . To compute  ${}^1\chi_1(G)$  and  $NM_2(G)$ , we need to partition the edge set into the sets of the form  $E_{p,q}$  and compute its cardinality. This information is presented in the Table 4. To have a good understanding of this computation, we have colored the edges with same color that lies in the same set  $E_{p,q}$  (see Fig. 4). Now using the values from the Table 4 in the definition of  ${}^1\chi_1(G)$  and  $NM_2(G)$ , we get

$$\begin{aligned} {}^1\chi_1(G) &= \sum_{vw \in E(G)} \frac{1}{\sqrt{S(v)S(w)}} \\ &= (8)\frac{1}{\sqrt{5 \times 4}} + (2(n-2))\frac{1}{\sqrt{5 \times 5}} + (4)\frac{1}{\sqrt{7 \times 5}} + (4(n-1))\frac{1}{\sqrt{8 \times 5}} \\ &\quad + (4(m-2))\frac{1}{\sqrt{6 \times 7}} + (2(m-2))\frac{1}{\sqrt{9 \times 7}} + (2(n-1))\frac{1}{\sqrt{8 \times 8}} \\ &\quad + (4(n-1))\frac{1}{\sqrt{8 \times 9}} + (m-3)(7n-9)\frac{1}{\sqrt{9 \times 9}} \\ &= \frac{4}{\sqrt{5}} + \frac{2(n-2)}{5} + \frac{4}{\sqrt{35}} + \frac{2(n-1)}{\sqrt{10}} + \frac{4(m-2)}{\sqrt{42}} + \frac{2(m-2)}{\sqrt{63}} \\ &\quad + \frac{n-1}{4} + \frac{2(n-1)}{\sqrt{18}} + \frac{(m-3)(7n-9)}{9} \\ &= \frac{7}{9}mn + (\frac{4}{\sqrt{42}} + \frac{2}{\sqrt{63}} - 1)m + (\frac{2}{\sqrt{10}} + \frac{2}{\sqrt{18}} - \frac{303}{180})n \\ &\quad + \frac{4}{\sqrt{5}} + \frac{4}{\sqrt{35}} - \frac{2}{\sqrt{18}} - \frac{8}{\sqrt{42}} - \frac{4}{\sqrt{63}} - \frac{2}{\sqrt{10}} + \frac{39}{20}. \end{aligned}$$

$$\begin{aligned} NM_2(G) &= \sum_{vw \in E(G)} S(v)S(w) \\ &= (8)(5 \times 4) + (2(n-2))(5 \times 5) + (4)(7 \times 5) + (4(n-1))(8 \times 5) \\ &\quad + (4(m-2))(6 \times 7) + (2(m-2))(9 \times 7) + (2(n-1))(8 \times 8) \\ &\quad + (4(n-1))(8 \times 9) + (m-3)(7n-9)(9 \times 9) \\ &= 160 + 50n - 100 + 140 + 160n - 160 + 168m - 336 + 126m - 252 \\ &\quad + 128n - 128 + 288n - 288 + 567mn - 1701n - 729m + 2187 \\ &= 567mn - 1075n - 435m + 1223. \end{aligned}$$

□

**Table 5** The edge partition of  $TUZC_6[m, n]$ .

$E_{p,q}$	Cardinality
$E_{6,7}$	4 m
$E_{7,9}$	2 m
$E_{9,9}$	6mn-10 m

**Theorem 2.** Let  $G$  be the graph of zigzag polyhex nanotube, then

$${}^1\chi_1(G) = \frac{2}{3}mn + \left(\frac{4}{\sqrt{42}} + \frac{2}{\sqrt{63}} - \frac{10}{9}\right)m.$$

$$NM_2(G) = 486mn - 516m.$$

**Proof.** The edge sets of the form  $E_{p,q}$  of  $G$  and their cardinalities are depicted in Table 5. To have a good understanding of this computation, we have colored the edges with same color that lies in the same set  $E_{p,q}$  (see Fig. 3). Now using the values from the Table 5 in the definition of  ${}^1\chi_1(G)$  and  $NM_2(G)$ , we get

$$\begin{aligned} {}^1\chi_1(G) &= \sum_{vw \in E(G)} \frac{1}{\sqrt{S(v)S(w)}} \\ &= (4m) \frac{1}{\sqrt{6 \times 7}} + (2m) \frac{1}{\sqrt{9 \times 7}} + (6mn - 10m) \frac{1}{\sqrt{9 \times 9}} \\ &= \frac{2}{3}mn + \left(\frac{4}{\sqrt{42}} + \frac{2}{\sqrt{63}} - \frac{10}{9}\right)m. \end{aligned}$$

$$\begin{aligned} NM_2(G) &= \sum_{vw \in E(G)} S(v)S(w) \\ &= (4m)(6 \times 7) + (2m)(9 \times 7) + (6mn - 10m)(9 \times 9) \\ &= 168m + 126m + 486mn - 810m \\ &= 486mn - 516m. \end{aligned}$$

□

**Theorem 3.** Let  $G$  be the graph of zigzag polyhex nanotorus, then

$${}^1\chi_1(G) = \frac{mn}{3}.$$

$$NM_2(G) = 243mn.$$

**Proof.** In  $G$ , all the edges are of the form  $E_{9,9}$ . Hence we have  $6mn$  edges in the set  $E_{9,9}$  and

$$\begin{aligned} {}^1\chi_1(G) &= \sum_{vw \in E(G)} \frac{1}{\sqrt{S(v)S(w)}} \\ &= (6mn) \frac{1}{\sqrt{9 \times 9}} \\ &= \frac{2mn}{3}. \end{aligned}$$

$$\begin{aligned} NM_2(G) &= \sum_{vw \in E(G)} S(v)S(w) \\ &= (6mn)(9 \times 9) \\ &= 486mn. \end{aligned}$$

□

### 3.2. Results for Nanosheets, Nanotubes and Nanotori covered by $C_4$ and $C_8$

A mutual decoration created by alternating squares  $C_4$  and octagons  $C_8$  is referred to as  $C_4C_8$  nanosheet.  $C_4C_8(S)$  and  $C_4C_8(R)$  nanosheets are obtained by the positioning of  $C_4$  squares and  $C_8$  octagons. We denote the nanosheet with  $n$  hexagon in each row and  $m$  hexagons in each column by  $C_4C_8(S)[m, n]$ . The order and size of  $C_4C_8(S)[m, n]$  nanosheet are  $8mn$  and  $12mn - 2m - 2n$  respectively. Similarly, the nanosheet with  $m$  squares in each row and  $n$  squares in each column is denoted by  $C_4C_8(R)[m, n]$ . The order and size of  $C_4C_8(S)[m, n]$  nanosheet are  $4mn + 4m + 4n + 4$  and  $6mn + 5m + 5n + 4$  respectively. Fig. 6 and Fig. 7 depicts the graphs of  $C_4C_8(R)[3, 5]$  and  $C_4C_8(S)[3, 4]$  nanosheets respectively. These nanosheets have uniform thickness and are important due to their novel characteristics such as stability and flexibility. Significant application of nanosheets can be viewed in sensors, filtration membranes and even conductive coatings (Turchanin et al., 2009). The chemical, mechanical and thermal stability of these nanosheets is equally strong. For more information on the computation of different topological indices of these nanosheets, we refer the readers to (Al-Fozan et al., 2014; Manuel et al., 2013; Arockiaraj et al., 2016). In the next Theorems, we compute the two connectivity indices of these nanosheets.

**Theorem 4.** Let  $G$  be the graph of  $C_4C_8(S)[m, n]$  nanosheet, then

$$\begin{aligned} {}^1\chi_1(G) &= \frac{4}{3}mn + \left(\frac{2}{\sqrt{10}} + \frac{2}{\sqrt{18}} - \frac{163}{180}\right)m + \left(\frac{2}{\sqrt{10}} + \frac{2}{\sqrt{18}} - \frac{163}{180}\right)n \\ &\quad + \frac{4}{\sqrt{5}} - \frac{4}{\sqrt{10}} - \frac{4}{\sqrt{18}} + \frac{61}{90}. \end{aligned}$$

$$NM_2(G) = 972mn - 508m - 508n + 168.$$

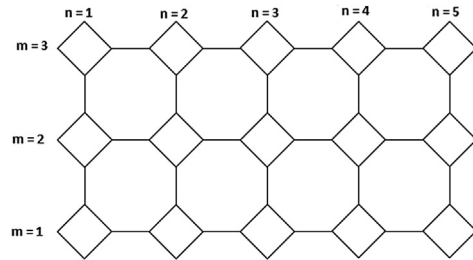


**Fig. 6** Structure of  $C_4C_8(R)[3, 5]$  nanosheet.

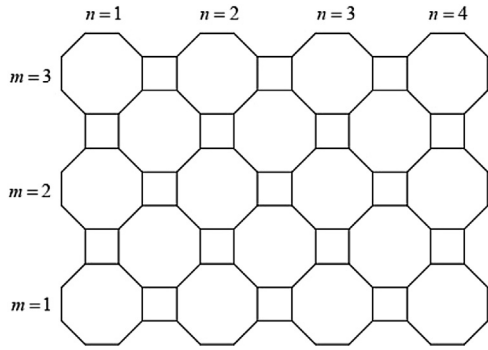


Fig. 7 Structure of  $C_4C_8(S)[3, 4]$  nanosheet.

Table 6 Edge partition of  $C_4C_8(S)[m, n]$

$E_{p,q}$	Cardinality
$E_{4,4}$	4
$E_{4,5}$	8
$E_{5,5}$	$2m + 2n - 8$
$E_{5,8}$	$4m + 4n - 8$
$E_{8,8}$	$2m + 2n - 4$
$E_{8,9}$	$4m + 4n - 8$
$E_{9,9}$	$12mn - 14m - 14n + 16$

**Proof.** The edge sets of the form  $E_{p,q}$  of  $G$  and their cardinalities are depicted in Table 6. Now using the values from the Table 6 in the definition of  ${}^1\chi_1(G)$  and  $NM_2(G)$ , we get

$$\begin{aligned}
 {}^1\chi_1(G) &= \sum_{vw \in E(G)} \frac{1}{\sqrt{S(v)S(w)}} \\
 &= (4) \frac{1}{\sqrt{4 \times 4}} + (8) \frac{1}{\sqrt{4 \times 5}} + (2m + 2n - 8) \frac{1}{\sqrt{5 \times 5}} \\
 &\quad + (4m + 4n - 8) \frac{1}{\sqrt{5 \times 8}} + (2m + 2n - 4) \frac{1}{\sqrt{8 \times 8}} \\
 &\quad + (4m + 4n - 8) \frac{1}{\sqrt{8 \times 9}} + (12mn - 14m - 14n + 16) \frac{1}{\sqrt{9 \times 9}} \\
 &= \frac{4}{3}mn + \left(\frac{2}{\sqrt{10}} + \frac{2}{\sqrt{18}} - \frac{163}{180}\right)m + \left(\frac{2}{\sqrt{10}} + \frac{2}{\sqrt{18}} - \frac{163}{180}\right)n \\
 &\quad + \frac{4}{\sqrt{5}} - \frac{4}{\sqrt{10}} - \frac{4}{\sqrt{18}} + \frac{61}{90}.
 \end{aligned}$$

$$\begin{aligned}
 NM_2(G) &= \sum_{vw \in E(G)} S(v)S(w) \\
 &= (4)(4 \times 4) + (8)(4 \times 5) + (2m + 2n - 8)(5 \times 5) + (4m + 4n - 8)(5 \times 8) \\
 &\quad + (2m + 2n - 4)(8 \times 8) + (4m + 4n - 8)(8 \times 9) \\
 &\quad + (12mn - 14m - 14n + 16)(9 \times 9) \\
 &= 972mn - 508m - 508n + 168.
 \end{aligned}$$

Table 7 Edge partition of  $C_4C_8(R)[m, n]$ .

$E_{p,q}$	Cardinality
$E_{5,5}$	4
$E_{5,8}$	8
$E_{6,8}$	$4m + 4n - 8$
$E_{8,8}$	$2m + 2n + 4$
$E_{8,9}$	$4m + 4n - 8$
$E_{9,9}$	$6mn - 5m - 5n + 4$

□

**Theorem 5.** Let  $G$  be the graph of  $C_4C_8(R)[m, n]$  nanosheet, then

$$\begin{aligned}
 {}^1\chi_1(G) &= \frac{2}{3}mn + \left(\frac{1}{\sqrt{3}} + \frac{2}{\sqrt{18}} - \frac{11}{36}\right)m + \left(\frac{1}{\sqrt{3}} + \frac{2}{\sqrt{18}} - \frac{11}{36}\right)n \\
 &\quad + \frac{4}{\sqrt{10}} - \frac{2}{\sqrt{3}} - \frac{4}{\sqrt{18}} + \frac{157}{90}.
 \end{aligned}$$

$$NM_2(G) = 486mn + 203m + 203n + 40.$$

**Proof.** The edge sets of the form  $E_{p,q}$  of  $G$  and their cardinalities are depicted in Table 7. Now using the values from the Table 7 in the definition of  ${}^1\chi_1(G)$  and  $NM_2(G)$ , we get

$$\begin{aligned}
 {}^1\chi_1(G) &= \sum_{vw \in E(G)} \frac{1}{\sqrt{S(v)S(w)}} \\
 &= (4) \frac{1}{\sqrt{5 \times 5}} + (8) \frac{1}{\sqrt{5 \times 8}} + (4m + 4n - 8) \frac{1}{\sqrt{6 \times 8}} \\
 &\quad + (2m + 2n + 4) \frac{1}{\sqrt{8 \times 8}} + (4m + 4n - 8) \frac{1}{\sqrt{8 \times 9}} \\
 &\quad + (6mn - 5m - 5n + 4) \frac{1}{\sqrt{9 \times 9}} \\
 &= \frac{2}{3}mn + \left(\frac{1}{\sqrt{3}} + \frac{2}{\sqrt{18}} - \frac{11}{36}\right)m + \left(\frac{1}{\sqrt{3}} + \frac{2}{\sqrt{18}} - \frac{11}{36}\right)n \\
 &\quad + \frac{4}{\sqrt{10}} - \frac{2}{\sqrt{3}} - \frac{4}{\sqrt{18}} + \frac{157}{90}.
 \end{aligned}$$

$$\begin{aligned}
 NM_2(G) &= \sum_{vw \in E(G)} S(v)S(w) \\
 &= (4)(5 \times 5) + (8)(5 \times 8) + (4m + 4n - 8)(6 \times 8) \\
 &\quad + (2m + 2n + 4)(8 \times 8) + (4m + 4n - 8)(8 \times 9) \\
 &\quad + (6mn - 5m - 5n + 4)(9 \times 9) \\
 &= 486mn + 203m + 203n + 40.
 \end{aligned}$$

□

The nanotube  $TUC_4C_8(S)[m, n]$  is obtained from the lattice  $C_4C_8(S)[m, n]$  by joining the dangling edges from the right to the leftmost vertex on the same row. The order and size of  $TUC_4C_8(S)[m, n]$  nanotube are  $8mn$  and  $12mn - 2n$  respectively. The graph of  $TUC_4C_8(S)[3, 4]$  nanotube is depicted in Fig. 8. Similarly, the nanotube  $TUC_4C_8(R)$  is obtained from the lattice  $C_4C_8(R)$  by joining the dangling edges from the right to the leftmost vertex on the same row. The order and

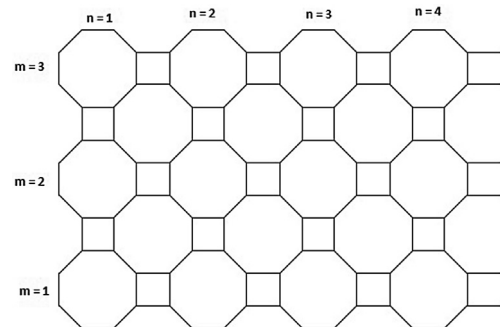


Fig. 8 Structure of  $TUC_4C_8(S)[3, 4]$ .

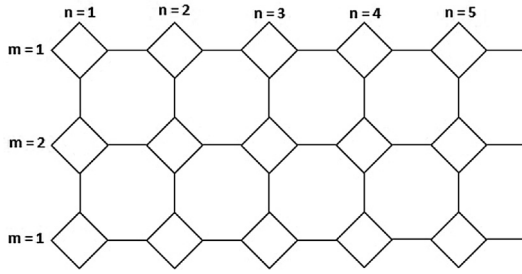


Fig. 9 2D structure of  $TUC_4C_8(R)[3, 5]$ .

Table 8 Edge partition of  $TUC_4C_8(S)[m, n]$ .

$E_{p,q}$	Cardinality
$E_{5,5}$	$2n$
$E_{5,8}$	$4n$
$E_{8,8}$	$2n$
$E_{8,9}$	$4n$
$E_{9,9}$	$12mn - 14n$

size of  $TUC_4C_8(R)[m, n]$  nanotube are  $4mn + 4m + 4n + 4$  and  $6mn + 6m + 5n + 5$  respectively. The graph of  $TUC_4C_8(R)[3, 5]$  nanotube is depicted in Fig. 9. Next we compute the connectivity indices of these two nanotubes.

**Theorem 6.** Let  $G$  be the graph of  $TUC_4C_8(S)[m, n]$  nanotube, then

$${}^1\chi_1(G) = \frac{4}{3}mn + \left(\frac{2}{\sqrt{10}} + \frac{2}{\sqrt{18}} - \frac{163}{180}\right)n.$$

$$NM_2(G) = 972mn - 508n.$$

**Proof.** The edge sets of the form  $E_{p,q}$  of  $G$  and their cardinalities are depicted in Table 8. Now using the values from the Table 8 in the definition of  ${}^1\chi_1(G)$  and  $NM_2(G)$ , we get

$$\begin{aligned} {}^1\chi_1(G) &= \sum_{vw \in E(G)} \frac{1}{\sqrt{S(v)S(w)}} \\ &= (2n) \frac{1}{\sqrt{5 \times 5}} + (4n) \frac{1}{\sqrt{5 \times 8}} + (2n) \frac{1}{\sqrt{8 \times 8}} + (4n) \frac{1}{\sqrt{8 \times 9}} \\ &\quad + (12mn - 14n) \frac{1}{\sqrt{9 \times 9}} \\ &= \frac{4}{3}mn + \left(\frac{2}{\sqrt{10}} + \frac{2}{\sqrt{18}} - \frac{163}{180}\right)n. \end{aligned}$$

Table 9 Edge partition of  $TUC_4C_8(R)[m, n]$ .

$E_{p,q}$	Cardinality
$E_{6,8}$	$4n + 4$
$E_{8,8}$	$2n + 2$
$E_{8,9}$	$4n + 4$
$E_{9,9}$	$6mn + 6m - 5n - 5$

$$\begin{aligned} NM_2(G) &= \sum_{vw \in E(G)} S(v)S(w) \\ &= (2n)(5 \times 5) + (4n)(5 \times 8) + (2n)(8 \times 8) + (4n)(8 \times 9) \\ &\quad + (12mn - 14n)(9 \times 9) \\ &= 972mn - 508n. \end{aligned}$$

□

**Theorem 7.** Let  $G$  be the graph of  $TUC_4C_8(R)[m, n]$  nanotube, then

$$\begin{aligned} {}^1\chi_1(G) &= \frac{2}{3}mn + \frac{2}{3}m + \left(\frac{1}{\sqrt{3}} + \frac{\sqrt{2}}{3} - \frac{11}{36}\right)n \\ &\quad + \frac{1}{\sqrt{3}} + \frac{\sqrt{2}}{3} - \frac{11}{36}. \end{aligned}$$

$$NM_2(G) = 486mn + 486m + 203n + 203.$$

**Proof.** The edge sets of the form  $E_{p,q}$  of  $G$  and their cardinalities are depicted in Table 9. Now using the values from the Table 9 in the definition of  ${}^1\chi_1(G)$  and  $NM_2(G)$ , we get

$$\begin{aligned} {}^1\chi_1(G) &= \sum_{vw \in E(G)} \frac{1}{\sqrt{S(v)S(w)}} \\ &= (4n + 4) \frac{1}{\sqrt{6 \times 8}} + (2n + 2) \frac{1}{\sqrt{8 \times 8}} + (4n + 4) \frac{1}{\sqrt{8 \times 9}} \\ &\quad + (6mn + 6m - 5n - 5) \frac{1}{\sqrt{9 \times 9}} \\ &= \frac{2}{3}mn + \frac{2}{3}m + \left(\frac{1}{\sqrt{3}} + \frac{\sqrt{2}}{3} - \frac{11}{36}\right)n \\ &\quad + \frac{1}{\sqrt{3}} + \frac{\sqrt{2}}{3} - \frac{11}{36}. \end{aligned}$$

$$\begin{aligned} NM_2(G) &= \sum_{vw \in E(G)} S(v)S(w) \\ &= (4n + 4)(6 \times 8) + (2n + 2)(8 \times 8) + (4n + 4)(8 \times 9) \\ &\quad + (6mn + 6m - 5n - 5)(9 \times 9) \\ &= 486mn + 486m + 203n + 203. \end{aligned}$$

□

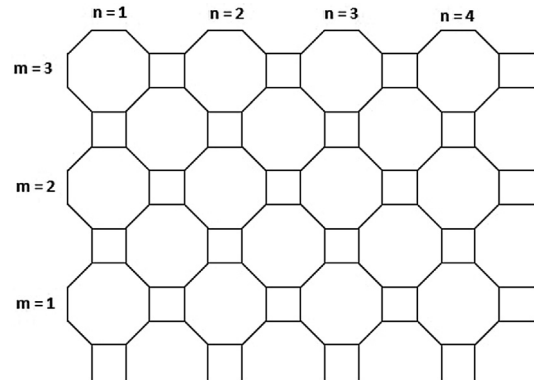
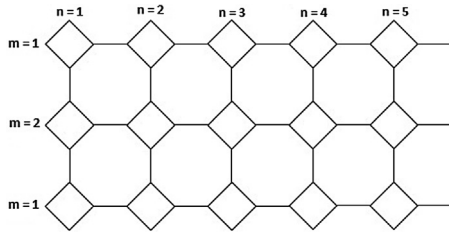


Fig. 10 Structure of  $TUC_4C_8(S)[3, 4]$ .



**Fig. 11** 2D structure of  $TUC_4C_8(R)[3, 5]$ .

The nanotori  $TC_4C_8(S)[m, n]$  is obtained from the nanotube  $TUC_4C_8(S)[m, n]$  by joining the dangling edges from the right to the leftmost vertex of same row and dangling edges from the bottom to the top vertices of the same column. The order and size of  $TC_4C_8(S)[m, n]$  nanotori are  $8mn$  and  $12mn$  respectively. The graph of  $TUC_4C_8(S)[3, 4]$  nanotube is depicted in Fig. 10. Similarly, the nanotube  $TUC_4C_8(R)$  is obtained from the nanotube  $TUC_4C_8(R)$  by joining the dangling edges from the right to the leftmost vertex on the same row and dangling edges from the bottom to the top vertices of the same column. The order and size of  $TC_4C_8(R)[m, n]$  nanotori are  $4mn + 4m + 4n + 4$  and  $6mn + m + n + 1$  respectively. The graph of  $TUC_4C_8(R)[3, 5]$  nanotori is depicted in Fig. 11. Next we compute the connectivity indices of these two nanotori.

**Theorem 8.** Let  $G$  and  $H$  be the graphs of  $TC_4C_8(S)[m, n]$  and  $TC_4C_8(R)[m, n]$  nanotori, then

$${}^1\chi_1(G) = \frac{4}{3}mn.$$

$$NM_2(G) = 972mn.$$

$${}^1\chi_1(H) = \frac{2}{3}mn + \frac{1}{9}m + \frac{1}{9}n + \frac{1}{9}.$$

$$NM_2(H) = 486mn + 81m + 81n + 81.$$

**Proof.** Note that all the edges of  $G$  and  $H$  belongs to the set  $E_{9,9}$ . The results follow from the definition of  ${}^1\chi_1$  and  $NM_2$ .  $\square$

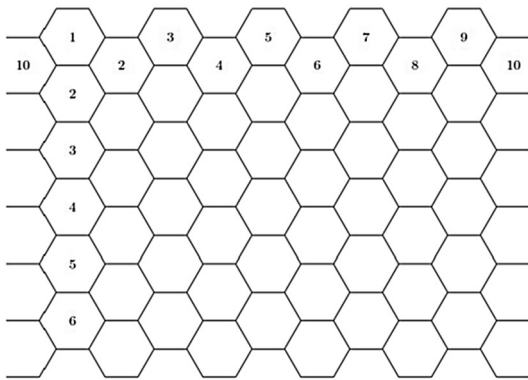


**Fig. 12** Armchair Polyhex Nanotube  $TUAC_6[m, n]$  for  $m = 10$  and  $n = 6$ .

**Table 10** Edge partitions of  $TUAC_6[m, n]$  (depends on degree summation of neighbors of end vertices).

$E_{p,q}$	Cardinality
$E_{5,5}$	$m$
$E_{5,8}$	$2m$
$E_{8,8}$	$m$
$E_{8,9}$	$2m$
$E_{9,9}$	$3mn - 4m$

### 3.3. Armchair Polyhex Nanotubes

An Armchair Polyhex Nanotube denoted by  $TUAC_6$  is obtained by rolling the graphene sheet into seamless tube such that horizontal axis of the tube is parallel to the carbon-carbon bonds. We use the notation  $TUAC_6[m, n]$  for the armchair polyhex nanotube with  $m$  and  $n$  hexagons in each row and column respectively. The graph of  $TUAC_6[10, 6]$  is depicted in Fig. 12. The order and size of  $TUAC_6[m, n]$  are  $2m(n + 1)$  and  $3mn + 2m$  respectively. Now, we compute the connectivity indices of  $TUAC_6[m, n]$ .

**Theorem 9.** Let  $G$  be the graph of  $TUAC_6[m, n]$  nanotube, then

$${}^1\chi_1(G) = \frac{1}{3}mn + \left(\frac{1}{\sqrt{10}} + \frac{1}{\sqrt{18}} - \frac{43}{360}\right)m.$$

$$NM_2(G) = 243mn - 11m.$$

**Proof.** The edge sets of the form  $E_{p,q}$  of  $G$  and their cardinalities are depicted in Table 10. Now using the values from the Table 10 in the definition of  ${}^1\chi_1(G)$  and  $NM_2(G)$ , we get

$$\begin{aligned} {}^1\chi_1(G) &= \sum_{vw \in E(G)} \frac{1}{\sqrt{S(v)S(w)}} \\ &= (m) \frac{1}{\sqrt{5 \times 5}} + (2m) \frac{1}{\sqrt{5 \times 8}} + (m) \frac{1}{\sqrt{8 \times 8}} + (2m) \frac{1}{\sqrt{8 \times 9}} \\ &\quad + (3mn - 4m) \frac{1}{\sqrt{9 \times 9}}. \\ &= \frac{1}{3}mn + \left(\frac{1}{\sqrt{10}} + \frac{1}{\sqrt{18}} - \frac{43}{360}\right)m. \end{aligned}$$

$$\begin{aligned} NM_2(G) &= \sum_{vw \in E(G)} S(v)S(w) \\ &= (m)(5 \times 5) + (2m)(5 \times 8) + (m)(8 \times 8) + (2m)(8 \times 9) \\ &\quad + (3mn - 4m)(9 \times 9) \\ &= 243mn - 11m. \end{aligned}$$

$\square$

## 4. Conclusion

In this paper, we have analyzed different nanotubes graphs such as zigzag nanotubes,  $C_4C_8(S)[m, n]$  nanostructure and armchair polyhex nanotubes  $TUAC_6[p, q]$  through newly introduced topological indices. Topological indices consequently determined can assist us with understanding their physical

characteristics, synthetic reactivity and natural exercises. These findings are precious and useful for scientists to comprehend profound behavior and construction of some carbon nanotubes. These findings are also significant contributors to the study of chemical graph theory, quantum chemistry, QSPR and QSAR.

## 5. Data availability statement

No data were used to support this study.

## Declaration of Competing Interest

The authors declare that they have no known competing financial interests or personal relationships that could have appeared to influence the work reported in this paper.

## References

- Al-Fozan, T., Manuel, P., Rajasingh, I., Rajan, R.S., 2014. Computing Szeged Index of Certain Nanosheets Using Partition Technique. *MATCH Commun. Math. Comput. Chem.* 72, 339–353.
- Arockiaraj, M., Clement, J., Shalini, A.J., 2016. Variants of Szeged index in certain chemical nanosheets. *Can. J. Chem.* 94 (7), 608–619.
- Balaban, A.T., 1979. Chemical graphs. XXXIV. Five new topological indices for the branching of tree-like graphs. *Theor. Chim. Acta* 53, 355–375.
- Balaban, A.T., 1988. Topological indices and their uses: a new approach for coding of alkanes. *J. Mol. Struct. (THEOCHEM)* 165, 243–253.
- Balaban, A.T., Motoc, I., Bonchev, D., Mekenyan, O., Charton, M., Motoc, I., 1983. Topological indices for structure activity relationship. In steric effort in drug design. *Topics Curr. Chem.* 114, 21–55.
- Bonchev, D., Kier, L.B., 1992. Topological atomic indices and the electronic changes in alkanes. *J. Math. Chem.* 9, 75–85.
- Chakrabarty, A., Zhang, L., Cavicchi, K.A., Weiss, R.A., Singha, N. K., 2015. Tailor-Made fluorinated copolymer/clay nanocomposite by cationic RAFT assisted pickering miniemulsion polymerization. *Langmuir* 31, 12472–12480.
- Diudea, M.V., Stefu, M., Párv, B., John, P.E., 2004. Wiener Index of Armchair Polyhex Nanotubes. *Croat. Chem. Acta* 77 (1–2), 111–115.
- Editorial, The many faces of nanotech, *Nat. Nanotechnol.* 2(10) (2007) 585. <https://doi.org/10.1038/nnano.2007.308>.
- Eliasi, M., Salehi, N., 2008. Schultz Index of Armchair Polyhex Nanotubes. *Int. J. Mol. Sci.* 9, 2016–2026.
- Eliasi, M., Taeri, B., 2008. Szeged index of armchair polyhex nanotubes. *MATCH Commun. Math. Comput. Chem.* 59, 437–450.
- Eliasi, M., Taeri, B., 2008. Hyper-Wiener index of zigzag polyhex nanotubes. *ANZIAM J.* 50 (1), 75–86.
- Farahani, M.R., 2012. Some Connectivity Indices and Zagreb Index of Polyhex Nanotubes. *Acta Chim. Slov.* 59, 779–783.
- Godsil, C., Royle, G., 2001. *Algebraic Graph Theory*. Springer-Verlag, New York.
- Gross, J.L., Yellen, J., 2000. *Graph Theory*. CRC Press, Boca Raton, Florida.
- Harary, F., 1969. *Graph Theory*. Addison-Wesley.
- Kanabur, R., 2018. On certain degree-based topological indices of armchair polyhex nanotubes. *Journal of Mathematical Nanoscience* 8 (1), 19–25.
- Liu, C., 2021. A note on domination number in maximal outerplanar graphs. *Discret. Appl. Math.* 293, 90–94.
- Mahmiani, A., Khormali, O., Iranmanesh, A., 2012. On the Edge Version of Geometric-Arithmetic Index. *Dig. J. Nanomater. Biostructures* 7 (2), 411–414.
- Manuel, P., Rajasingh, I., Rajan, B., Rajan, R.S., 2013. A new approach to compute Wiener index. *J. Comput. Theor. Nanosci.* 10, 1515–1521.
- Monajjemi, M., Mohammadinasab, E., Shafiei, F., 2008. Topological relationship between electric quadrupole, hexadecapole moments, energy and Padmakar-Ivan index in armchair polyhex nanotubes TUVC6[2p, q]. *J. Phys. Theor. Chem.* 4 (4), 217–222.
- Qiad, Z., Zhang, L., Stein, G.E., Cavicchi, K.A., Vogt, B.D., 2014. Unidirectional alignment of block copolymer films induced by expansion of a permeable elastomer during solvent vapor annealing. *Macromolecules* 47, 1109–1116.
- Randić, M., 1991. Novel graph theoretical approach to heteroatoms in quantitative structure-activity relationship. *Chemometrics Intel. Lab. Systems* 10, 213–227.
- Réti, T., Ali, A., Varga, P., Bitay, E., 2019. Some properties of the neighborhood first Zagreb index. *Discrete Math. Lett.* 2, 10–17.
- Shao, Z., Wu, P., Zhang, X., Dimitrov, D., 2018. Jia-Bao Liu, On the maximum ABC index of graphs with prescribed size and without pendent vertices. *IEEE Access* 6, 27604–27616.
- Stover, D., Normile, D., 1993. Buckytubes. *Pop. Sci.* 240 (4), 31.
- Tavakoli, M., Rahbarnia, F., Ashrafi, A.R., 2013. Note on strong product of graphs, Kragujev. *J. Math.* 37 (1), 187–193.
- Toropov, A.A., Toropova, A.P., Ismailov, T.T., Voropaeva, N.L., Ruban, I.N., 1997. Extended molecular connectivity: predication of boiling points of alkanes. *J. Struct. Chem.* 38, 965–969.
- Trinajstić, N., 1992. *Chemical Graph Theory*. CRC Press.
- Turchanin, A., Beyer, A., Notbohm, C.T., Zhang, X., Stosch, R., Sologubenko, A., Mayer, J., Hinze, P., Weimann, T., Golzahuser, A., 2009. *Adv. Mater.* 21, 1233–1237.
- Wang, S., Zhou, B., 2014. On the first extended zeroth-order connectivity index of trees. *Iran. J. Sci. Tech. A* 38, 213–219.
- Wang, Q.H., Yan, M., Chang, R.P.H., 2001. Flat panel display prototype using gated carbon nanotube field emitters. *Appl. Phys. Lett.* 78, 1294.
- Xiao, L., Chen, Sh., Guo, Zh., Chen, Q., 2010. The Geometric-Arithmetic Index of Benzenoid Systems and Phenylenes. *Int. J. Contemp. Math. Sciences.* 5 (45), 2225–2230.
- Zhang, L., Kucera, L.R., Ummadisetty, S., Nykaza, J.R., Elabd, Y.A., Storey, R.F., Cavicchi, K.A., Weiss, R.A., 2014. Supramolecular multiblock polystyrene-polyisobutylene copolymers via ionic interactions. *Macromolecules* 47, 4387–4396.
- X. Zhang, H.M. Awais, M. Javaid, M.K. Siddiqui, Multiplicative Zagreb Indices of Molecular Graphs, *J. Chem.* (2019) ArticleID: 5294198, 1–20. DOI: 10.1155/2019/5294198.
- X. Zhang, Abdul Rauf, M. Ishtiaq, M.K. Siddiqui, Mehwish Hussain Muhammad, On Degree Based Topological Properties of Two Carbon Nanotubes, *POLYCYCL AROMAT COMP* 2020 1–19. DOI:10.1080/10406638.2020.1753221.
- Zhou, B., Trinajstić, N., 2009. On extended connectivity indices. *J. Math. Chem.* 46, 1172–1180.